Article

Relationship of fragmentation of cylindrical rock specimen and incident underwater shock wave

Woo-Jin Jung*, Yuji Ogata*, Shiro Kubota**, Hideki Shimada**, and Kikuo Matsui**

This paper presents a new technique to estimate the behavior of the dynamic fracture of rock under explosive loading. The explosive material is used as the explosion source, and a pipe filled with water is arranged between the explosive and the cylindrical rock specimen. After the explosion, the detonation wave interacts with water and the underwater shock wave is generated in the pipe. Because the underwater shock wave attenuates with its propagation, the impact strength of the shock wave into the rock specimen can be easily adjusted by changing the length of the pipe. The free surface velocity at the end of the rock specimen and the position of cracks on the rock surface are observed by using a laser vibration meter and high-speed camera, respectively. The results of the fracture test for Kimachi sandstone are discussed. Moreover, the numerical simulation was carried out to understand the behavior of underwater shock wave generated by underwater explosion of the explosive. The 2D hydrodynamic code based on ALE finite difference scheme was employed. In the case of the fracture test with 50mm water pipe, the incident underwater shock wave into the cylindrical rock specimen has an irregular pressure distribution near the shock front.

1. Introduction

Explosive energy has been utilized for blasting, which is necessary for mining and quarrying operations and civil engineering applications. Because structures that were built in during the boom year have a relatively short lifespan, large numbers of these structures will be required to be demolished in the near future in Japan[1]. Because of its low cost and high efficiency, the demolition, which utilizes blasting, may become one of the most powerful methods if the technique is effective. In order to promote blasting efficiency and to establish effective blasting demolition techniques, it is important to know the mechanism of the dynamic fracture process on rock or construction materials. The fragmentation by blasting is the joint action of gaseous pressure and stress waves[2]. Because the stress wave greatly depends on the fracture conditions near the explosion source, the fragmentation near the free surface by the reflection of the stress wave also depends on it. Therefore, it is necessary to consider the experiments that can simultaneously estimate the fragmentation conditions both near the explosion source and near the free surface. The experimental and numerical studies were conducted to understand the behavior of the dynamic fracture of the rock under the explosive loading. In the experimental study, a new technique, which include underwater explosion as dynamic loading, was proposed. The explosive material is used as the explosion source, and a pipe filled with water is arranged between the explosive and the cylindrical rock specimen. After the explosion, the detonation wave interacts with water and the

Received : May 17, 2002
Accepted : August 16, 2002
*National Institute of Advanced Industrial Science and Technology,
16-1 Onogawa, Tsukuba, Ibaraki 305-8569, JAPAN
Tel. & Fax 81-298-61-8138, e-mail jung-wj@aist.go.jp
**Department of Earth Resources Engineering, Kyushu University,
6-10-1, Hakozaki, Higashi-ku, Fukuoka, 812-8581, JAPAN
Tel. 81-92-642-3614, e-mail Kubota@mine.kyushu-u.ac.jp

underwater shock wave is generated in the pipe. Because the underwater shock wave attenuates with its propagation, the impact strength of the shock wave into the rock specimen can be easily adjusted by changing the length of the water pipe. The main purpose of this fracture test is to collect the experimental data on the behaviors of dynamic fracture of the rock. We would like to provide these experimental data, which can confirm the validities of the related numerical simulations or fracture models for the rock materials. In addition, one of the aims of this test is to estimate the dynamic tensile strength of the rock for a wide range of a strain rate utilizing Hopkinson's effect. Therefore, the free surface velocity at the end of a rock specimen and the position of cracks on the rock surface are observed by using a laser vibration meter and high-speed camera, respectively. In the numerical study, we carried out the numerical simulation to understand the behavior of underwater shock wave generated by underwater explosion of the explosive. The 2D hydrodynamic code based on ALE finite difference scheme was employed. The JWL equation of sate was used for the detonation products, and Hugoniot Mie-Gruneisen type equation of sate was used for water and PMMA. From the results of the fracture test for Kimachi sandstone and the numerical simulation of the underwater shock wave, we will discuss the validity of this shock loading test.

2. Experimental set up

Fig. 1 shows the experimental set up for the proposed fracture test. During the fracture process

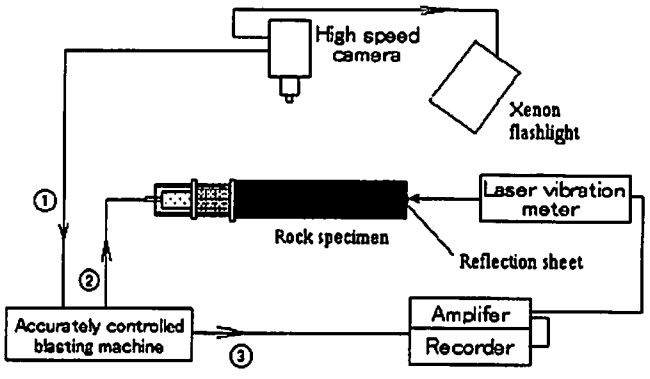

Fig. 1 Experimental set up for proposed fracture test of rock utilizing underwater shock wave.

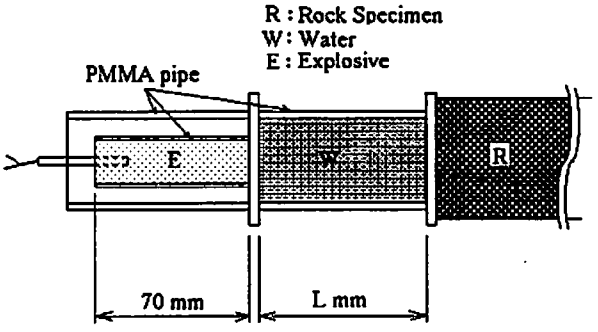

Fig. 2 The part of the explosion source for the proposed fracture test.

of the rock, the free surface velocity and the fracture part near the free surface were observed by a laser vibration meter (OFV-300; made by Polytec) and high speed camera (model 124 framing type camera; made by Cordin). The light source for a high speed camera uses a Xenon flashlight. The precise detonator was used to control the initiation time of the explosive by using an accurately controlled blasting machine, which was made by Nihon Kayaku Co. Ltd. Fig. 2 shows the part of the explosion source for the proposed fracture test. For the explosion source, the emulsion explosive was used. Because the detonation product rapidly expands and obstructs the view of the high speed camera, the explosive is set in the double layer pipe. After the explosion by the precise detonator, the detonation wave interacts with water, and the underwater shock wave generates in the pipe filled with water. Because the underwater shock wave attenuates with its propagation, the impact strength of the shock wave into the rock specimen can be easily adjusted by changing the length of the pipe. In this experiment the length of the water pipe was varied as 30, 50, 70, 100, 150, 200 and 300mm. Kimachi sandstone was used as the rock specimen with 60mm of diameter and 300mm of length. Arrival time at the free surface of the stress wave from the initiation of emulsion can be roughly estimated in the following for the trigger setting. The transit time of the detonation wave in the explosive pipe is about 18μs estimated by 4000m/s average detonation velocity and 70mm length of the pipe. The underwater shock wave spends 25μs to pass through the water part estimated by the

2000m/s average velocity of the underwater shock wave and the 50mm length of the water pipe. By using the average velocity of the 2700m/s longitudinal wave of Kimachi sandstone, it is understood that the stress wave pass through the rock specimen about 110μs.

3. Estimation methods for the dynamic tensile strength

Under the action of one-dimensional shock loading, the stress that acted on the material is given by

$$\sigma = \rho c_p v \tag{1}$$

where ρ is density, c_p the velocity of elastic wave and v the particle velocity of the material. Hino[3)4)] showed that reflection of the shock wave at the free surface causes the fracture of the rock near the free surface and proposed the original method for determining the dynamic tensile strength of the rock materials. Fig. 3 indicates the conceptual

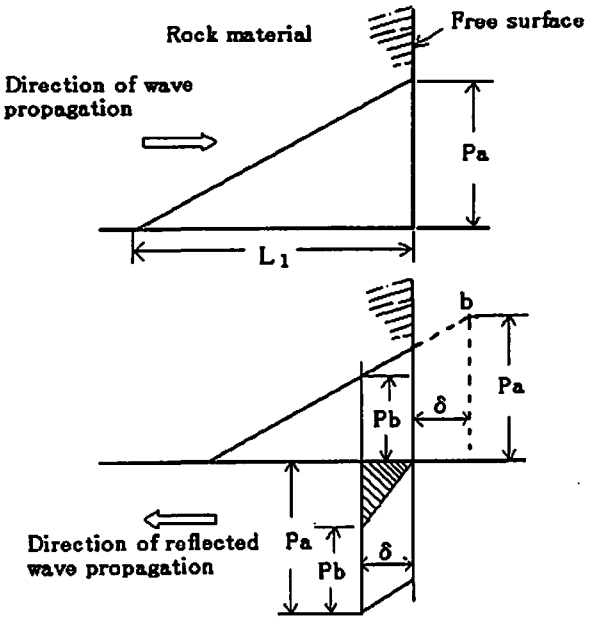

Fig. 3 Conceptual diagram for the estimation method of dynamic tensile strength (Hino 1956).

diagram for the estimation method of dynamic tensile strength proposed by Hino. In this figure the upper diagram corresponds to the stress distribution when one-dimensional shock wave reaches the free surface, and the lower one corresponds when spalling occurs. If there is no free surface, the shock wave travels into the rock material which is shown as a broken line in this figure. However due to the existence of the free surface, the shock wave goes back to the opposite side as a solid line. The tensile stress near the free surface can be estimated by using both compressive and tensile components, $P_a+(-P_b)$. The '+' corresponds to tension. Finally when the sum of these components exceeds the dynamic tensile strength S_d, the fracture of the rock material just occurs. Therefore S_d can be expressed as follows:

$$S_d = 2Pa\frac{\delta}{L_1} \tag{2}$$

where δ is the distance from the free surface to the fracture surface and L_1 the pulse width of the stress wave. In the above concept, there are three important assumptions: 1) the phenomena is a one-dimension, 2) the stress wave is a triangle pulse and a shock wave 3) the stress wave, which travels in the materials by free surface, is steady near the free surface. From these assumptions, L_1 can be obtained by the number of slabs N as in the following equation.

$$N = \frac{L_1}{2\delta} = \frac{P_a}{S_d} \tag{3}$$

Ma *et al.*[5)] also indicated the prediction method for dynamic tensile strength of rock materials. History of the free surface velocity $v_f(t)$ is continually measured by using a laser vibration meter and is converted to stress history at an inner point of the material. Fig. 4 shows the conceptual diagram for determining the dynamic tensile

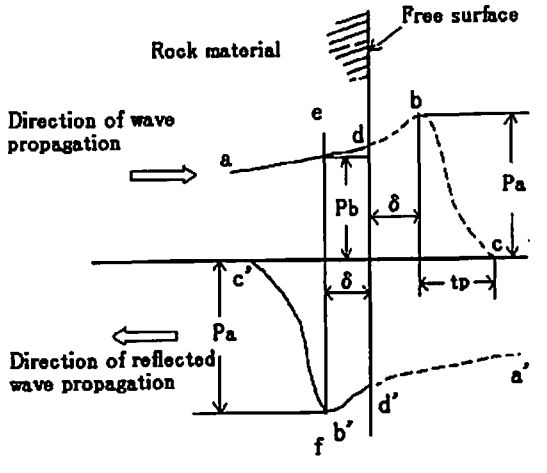

Fig. 4 Conceptual diagram for the estimation method of dynamic tensile strength (Ma et. al 1998).

strength. In this case the assumption 2) has not been considered because the history of the stress wave is obtained directly from the experiment. Instead, one assumption is added; that the fracture occurs when the peak of the stress wave for the tensile component arrives at the fracture surface. From the free surface approximation, the peak stress of the tensile component is $\bar{n}c_p\, v_f(t_p)\,/\,2$. The dynamic tensile strength is given by

$$S_d = \rho c_p \frac{v(t_p) - v(t_p + 2\Delta t)}{2} \quad (4)$$

The first term corresponds to the compressive component, and Δt is δ / c_p One of the purposes of this fracture test is to estimate the dynamic tensile strength of the rock according to above estimation methods, and we will discuss the relation between the results of the test and the assumptions in the methods.

4. Numerical simulation of underwater shock wave

To understand the behavior of underwater shock wave generated by underwater explosion of the explosive, we carried out the numerical simulation. In this calculation, the developed arbitrary Lagrangian Eulerian method[6] was used. The governing equation is based on mass, momentum and energy conservation laws. In addition, the equations of state for materials are necessary. For the explosive, the JWL form equation of state[7] was used to describe the expansion of the detonation products. The expression is given by

$$P = A\left(1 - \frac{\omega}{R_1 \rho}\right)\exp(-R_1\zeta) + B\left(1 - \frac{\omega}{R_2 \rho}\right)\exp(-R_2\zeta) + \frac{\omega}{\rho} E \quad (5)$$

where ζ is the ratio of the density of explosive to the density of detonation gas products and, ρ_o density of explosive. The coefficients A, B, C, R_1, R_2, which are constants have been determined by the expansion tube tests. For water and PMMA, the Mie-Grunisen equation of state was used. Because the equation of state of the emulsion explosive has not been formulated at present, here, the explosive of Aquanal whose detonation characteristics are similar to the emulsion explosive was used instead. The characteristics of Aquanal are shown in Table 1[8]. The constants for the Mie-Grunisen equations of state are shown in Table 2[9]. Fig. 5 indicates the calculation field. The computing grid sizes for calculation field about 5mm×5mm and the dimension of the calculation field was the same that of the experiments. The time step was determined by CFL condition with safety factor 0.1.

Table 1. The characteristics of Aquanal explosive (Jung *et al.*).

Composition	Density (kg/m^3)	Detonation velocity(m/s)	Pcj (GPa)
Slurry + Al	1430	3700	5.5

Table 2. The constants of Mie-Grunisen EOS (Jung *et al.*).

Material	Density (kg/m^3)	C_0 (m/s)	S	Γ
Water	1000	1483	2.0	1.0
PMMA	1181	2260	1.816	0.75

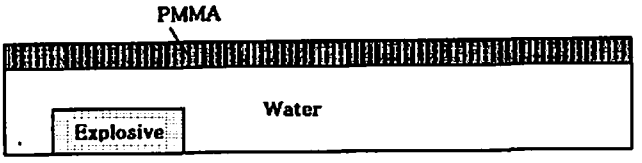

Fig. 5 Calculation field. (Jung etal.)

5. Results and discussion

5.1 Numerical results for the propagation of the underwater shock wave

In this fracture test, difference of configuration on incident underwater shock into rock specimen must be greatly related the difference of tendency on fracture situation on each experimental condition. Therefore we calculate the propagation process of the underwater shock wave generated by underwater explosion of explosive. Fig.6 shows the pressure distributions of the underwater shock wave along the axis obtained by numerical simulation. The time is counted from the incidence of detonation wave into the water. Fig. 6(a) corresponds to pressure distribution near the explosion source, and (b) is that 20mm-60mm from the initial interface. The strength of the underwater shock wave caused by interaction of detonation products and the water rapidly depressed to 0.5GPa while it propagates only 30mm. At this time the underwater shock front had a bending shape. When the underwater shock wave

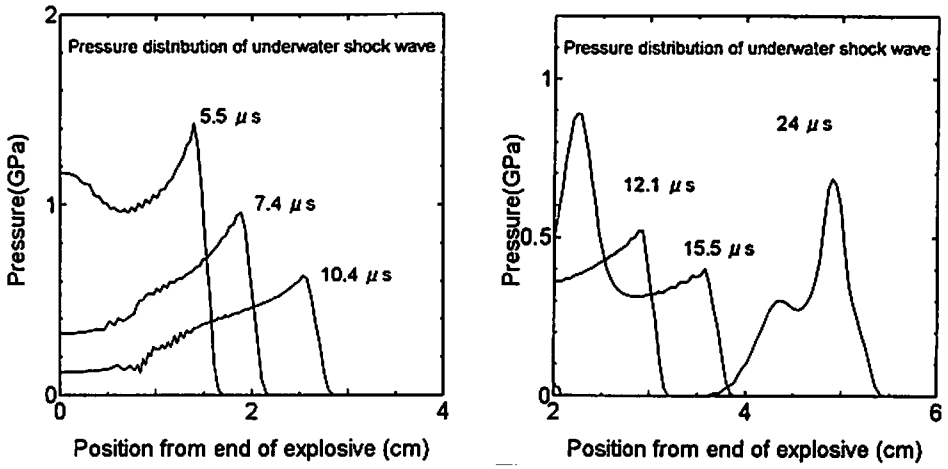

(a) near the explosion source

(b) 20mm~60mm from the explosion source

Fig. 6 Calculation results for propagation of underwater shock wave with pressure distributions along an axis.

propagates about 40mm (Fig. 6(b) 15.5μ), the second wave appears behind the shock front. The existence of the second wave shows that the reflection wave caused by interaction of the underwater shock wave and PMMA pipe reached the axis. After the shock front propagates about 50mm, the second wave catch up with the shock front. From the numerical results, it can be seen that in the case of the fracture test with 30mm water pipe, the shock loading to the rock specimen is not plane wave, and in the case of the fracture test with 50mm water pipe, the incident underwater shock wave into the cylindrical rock specimen has irregular pressure distribution near the shock front.

5.2 Experimental results

In the cases of 30mm and 50mm water pipe, the end of the rock specimen at the explosion side was broken into pieces over wide range, and the fracture part could not be recovered. While in the case of the 70mm water pipe, the fractured part near the explosion source had a few parts in the periphery of the specimen, and when the length of the water pipe was set more than 100mm water pipe, there is no damage near the explosion side of the recovered rock specimen. Under such condition, the stress wave near the free face is unrelated to the fracture conditions near the explosion source. The size of fragment near the free end increases as length of water pipe decreases with less than 70mm water pipe and also increases as length of water pipe increases with more than 70mm. Fig. 7 shows the profile of the free surface velocity

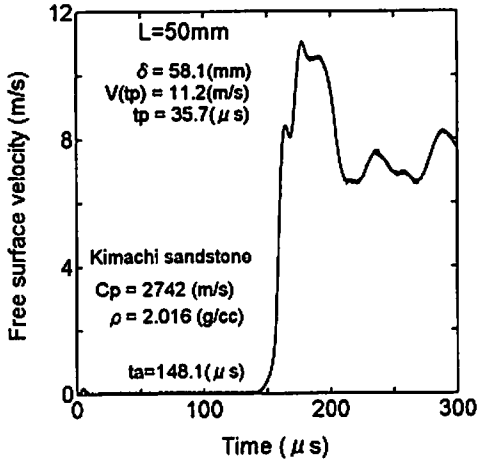

Fig. 7 Typical profile of the free surface velocity in the case of the 50mm water pipe.

obtained by the laser vibration meter in the case of the 50mm water pipe. In this figure, δ is the thickness of the fragment, $V(t_p)$ is the maximum velocity of the free surface and t_p is the time needed to reach the maximum velocity. Let us consider the meaning of this velocity profile. Just after the stress wave arrived at the free surface, the velocity starts to increase. The maximum velocity of this profile corresponds to the peak of the stress wave, which propagates in the material, and then the

velocity gradually decreases with the degradation of the stress. If the fragmentation of the material does not occur, the velocity slowly approaches 0 to stop the free surface. When the fracture of the rock specimen begins to occur near the free surface, we can find the remarkable change in velocity in the profile. After the fragmentation is accomplished, a fragment moves with nearly uniform velocity. Because the observation point is the free surface of the rock specimen, the time, which the tensile component of the stress wave propagate from the free surface to the fracture surface is $\Delta t\ (=\delta / c_p)$. The time in which the disturbance, due to the fracture of the specimen, arrives at the free surface is also Δt. Now we note the assumption, the fracture of the specimen occurs when the peak of the stress wave for the tensile component just arrives at the fracture surface. If the assumption is valid, there must be no remarkable change in the velocity for the profile during $2\Delta t$ from the maximum velocity. However, we can see the remarkable change within $2\Delta t$. Fig. 8 indicates the relationship of maximum free surface velocity and the length of water pipe. The maximum velocity decreases as the pipe length increases, and its decreasing rate gradually is dropping.

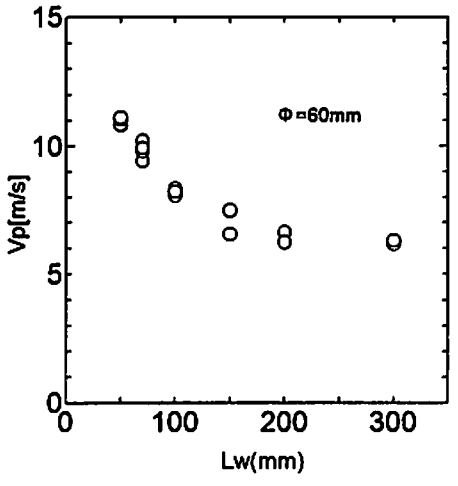

Fig. 8 Maximum free surface velocity of rock specimen vs. length of the pipe.

6. Aknowledgments

This study was supported by JSPS fellow ship program and the foundation for the promotion of the industrial explosives technology. Their support is gratefully acknowledged.

References

1) Ma, G., Miyake, A., Ogawa, T., Ogata, Y., Seto, M. and Katsuyama, K., 1998a. "Numerical Investigation on breakage behavior of reinforced concrete by blasting demolition", Journal of the Japan explosives society 59,2, pp.93-102

2) Bhandari, S., 1997, "Engineering rock blasting operations", A.A.Balkema, Rotterdam, Brookfield

3) Hino, K., 1956a, "Fragmentation of rock through blasting", Journal of the industrial explosives society, Japan 17, 1, pp.2-11

4) Hino, K., 1956b, "Velocity of rock fragments and shape of shock wave", Journal of the industrial explosives society, Japan 17, 4, pp.236-241

5) Ma G., Miyake A., Ogawa T., Wada Y., Ogata Y., Seto M. and Katsuyama K., 1998b. "Study on the Numerical Investigation on breakage behavior of reinforced concrete by blasting demolition", Journal of the Japan explosives society 59,2, pp.49-56

6) Hirt C.W., Amsden A.A. and Cook J.L., 1974, "An arbitrary Lagrangian-Eulerian computing method for all flow speeds", Journal of Computational Physics 14, 227-253

7) Lee E.L., Finger M., Collins W., 1973, Lawrence Livermore National Labolatory, Rept–UCID - 16189

8) Hornberg H., 1986, "Determination of fume states parameters from expansion measurements of meal tube", Propellants, Explosives, Pyrotechnics, 11, 23-31

9) Marsh S.P., 1980, "LASL Shock Hugoniot Data", University of California Press, Bekeley, CA, USA